

1 **NDEL1-PDGFRB FUSION GENE IN A MYELOID MALIGNANCY WITH**  
2 **EOSINOPHILIA ASSOCIATED WITH RESISTANCE TO TYROSINE KINASE**  
3 **INHIBITORS**  
4

5 Short title: TKI-resistant myeloid malignancy with NDEL1-PDGFRB

6 Konstantin Byrgazov<sup>1</sup>, Maria Gorna<sup>2</sup>, Gregor Hoermann<sup>3</sup>, Margit Koenig<sup>1</sup>, Raphael Ulreich<sup>4</sup>, Martin  
7 Benesch<sup>4</sup>, Volker Strenger<sup>4</sup>, Herwig Lackner<sup>4</sup>, Wolfgang Schwinger<sup>4</sup>, Petra Sovinz<sup>4</sup>, Oskar A.Haas<sup>1</sup>,  
8 Marry van den Heuvel-Eibrink<sup>5</sup>, Charlotte M.Niemeyer<sup>6</sup>, Oliver Hantschel<sup>7</sup>, Peter Valent<sup>8</sup>, Giulio  
9 Superti-Furga<sup>2</sup>, Christian Urban<sup>4</sup>, Michael N.Dworzak<sup>1,9</sup>, Thomas Lion<sup>1,10\*</sup>

10 <sup>1</sup> - Children's Cancer Research Institute; Vienna, 1090; Austria.

11 <sup>2</sup> - Center for Molecular Medicine (CeMM) of the Austrian Academy of Sciences; Vienna, 1090; Austria.

12 <sup>3</sup> - Department of Laboratory Medicine; Medical University of Vienna; Vienna, 1090; Austria.

13 <sup>4</sup> - Department of Pediatrics and Adolescent Medicine; Medical University of Graz; Graz, 8036; Austria.

14 <sup>5</sup> - Erasmus MC-Sophia Children's Hospital; Pediatric Oncology/Hematology; Rotterdam, 3015, and Princess  
15 Máxima Center for Pediatric Oncology; Utrecht, 3584; The Netherlands.

16 <sup>6</sup> - Department of Pediatrics and Adolescent Medicine; University of Freiburg; Freiburg, 79106; Germany.

17 <sup>7</sup> - Swiss Institute for Experimental Cancer Research (ISREC); School of Life Sciences; École Polytechnique  
18 Fédérale de Lausanne (EPFL); Lausanne, CH-1015; Switzerland.

19 <sup>8</sup> - Department of Internal Medicine I; Division of Hematology and Hemostaseology and Ludwig Boltzmann  
20 Cluster Oncology; Medical University of Vienna; Vienna, 1090; Austria.

21 <sup>9</sup> - St. Anna Children's Hospital; Vienna, 1090; Austria.

22 <sup>10</sup> -Department of Pediatrics, Medical University of Vienna; Vienna, 1090; Austria.

23 \*Correspondence: thomas.lion@ccri.at

24 We have identified a novel fusion gene *NDEL1-PDGFRB* in an 18-month old child  
25 with a myeloid neoplasm and eosinophilia<sup>1, 2</sup>. In contrast to earlier data on fusion  
26 genes involving *PDGFRB* in myeloid malignancies, which were generally responsive  
27 to treatment with imatinib<sup>3</sup>, the patient presented became refractory to both imatinib  
28 and nilotinib. Sequencing of a pertinent gene panel including *NRAS*, *KRAS*, *NF1*,  
29 *PTPN11*, *CBL*, *FLT3*, *c-KIT*, *PDGFRA*, *CSF1R*, *CSF3R*, *SF3B1*, *SRSF2*, *ZRSR2*,  
30 *SH2B3*, *RUNX1*, *EZH2*, *ASXL1*, *SETBP1*, *DNMT3A*, *TET2*, *PTEN* at the time of  
31 diagnosis and both relapses revealed no mutations. However, sequence analysis of  
32 the entire tyrosine kinase domain (TKD) of *PDGFRB* revealed the D850E mutation in  
33 the activation loop (A-loop). This mutation was identified in peripheral blood (PB) and  
34 bone marrow (BM) specimens from both relapses in virtually all cells belonging to the  
35 leukemic clone, but was undetectable in the diagnostic PB or BM. In order to  
36 elucidate the structural effects mediated by the D850E mutation in the PDGFR $\beta$  TKD,  
37 we have generated structure models of the kinase domain both in active (*DFG-in*)  
38 and inactive (*DFG-out*) conformations, which interact preferentially with type-I and  
39 type-II TKIs, respectively (Fig.1)<sup>4</sup>. Since the structure of PDGFR $\beta$  TKD at the level of  
40 atomic resolution is not yet available, we have modelled the kinase domain on the  
41 basis of crystallographic structures of closely related homologous proteins including  
42 c-KIT, CSF-1R and VEGFR2. All structural models indicated that the observed type-II  
43 TKI resistance of cells expressing the D850E mutation in *NDEL1-PDGFR $\beta$*  was  
44 conceivably related to stabilization of the A-loop in the active conformation. In this  
45 conformation, the DFG triad serving as a hypomochlion for the A-loop, adopts the so-  
46 called *DFG-in* position<sup>5</sup>. The modelled structure of the inactive *DFG-out* conformation  
47 (Fig.1A;orange) revealed the typical auto-inhibitory interaction between D850 and the  
48 amino acid at the +3 position, R853, which is commonly observed in inactive TKDs of  
49 other receptor tyrosine kinases (RTKs) from the PDGFR family, and is believed to

50 stabilize the A-loop in the inactive conformation (Fig.1B)<sup>6-8</sup>. However, modelling of  
51 the mutant PDGFR $\beta$  TKD in the inactive conformation could not explain the  
52 resistance to type-II TKIs and the enhanced kinase activity addressed below,  
53 because the negatively charged E850 is also able to form a salt bridge with the  
54 positively charged side chain of R853. By contrast, the DFG-*in* model suggested the  
55 occurrence of two intriguing amino acid interactions upon transition of the A-loop from  
56 inactive to the active state (Fig.1A;green). One interaction implicated the negatively  
57 charged D850 and the positively charged, conserved H657 in the  $\alpha$ C-helix (Fig.1C),  
58 which is expected to stabilize the A-loop in the active conformation<sup>9</sup>. This interaction  
59 can be further enhanced by the D850E mutation, because the longer side chain of  
60 glutamate in comparison to aspartate brings the negatively charged carboxylic group  
61 1.1 Å closer to the positively charged histidine. This increases the stability of the A-  
62 loop in the active conformation (Fig.1D), because the forces of electrostatic  
63 interaction between opposite charges increase with the second power of decreasing  
64 distance, and become largely ineffective at distances exceeding 4.5 Å<sup>10</sup>. The  
65 structural model also suggested that the mutation H657K would have an effect similar  
66 to the mutation D850E in terms of stabilizing the active conformation (Fig.1E). The  
67 other interaction involved R853 and E946 in the C-lobe of the TKD. The +3 position  
68 to D850 is one of the least conserved positions in the A-loop of RTKs from the  
69 PDGFR family (Fig.1H), and the arginine at this position in PDGFR $\beta$  (R853) has the  
70 longest side chain among all members. The DFG-*in* model suggested that the  
71 positively charged side chain of R853 can reach a distance of approximately 2.7 Å to  
72 the negatively charged carboxyl group of E946, which may facilitate electrostatic  
73 bonds and provide additional stabilization of the DFG-*in* conformation of the PDGFR $\beta$   
74 TKD. The structural model therefore suggested resistance of *NDEL1-PDGFRB* with  
75 the D850E mutation to type-II TKIs, which can only bind to the inactive conformation

76 of the PDGFR $\beta$  TKD, but indicated sensitivity to type-I TKIs binding to the active  
77 conformation. To address the predictions provided by the protein model, we have  
78 introduced several mutations affecting the aforementioned interactions, and tested  
79 the sensitivity of generated constructs against a panel of TKIs.

80 To assess the oncogenic potential of the newly identified fusion gene, the murine cell  
81 line Ba/F3 was stably transduced with wildtype or mutant *NDEL1-PDGFRB*  
82 constructs by employing a transposon-based system<sup>11</sup>. In addition to the D850E  
83 mutation observed in the patient, a construct carrying the H657K mutation was  
84 generated. This mutation was expected to strengthen the electrostatic interaction  
85 between D850 and the  $\alpha$ C-helix, thus stabilizing the DFG-*in* conformation of the  
86 PDGFR $\beta$  TKD (Fig.1E). In order to determine the influence of R853 in the PDGFR $\beta$   
87 TKD on the kinase activity and TKI-sensitivity, constructs carrying R853H were  
88 generated (Fig.1G). Ba/F3 cells expressing the H657K and D850E mutant versions of  
89 *NDEL1-PDGFRB* displayed an elevated *in vitro* kinase activity, whereas constructs  
90 with the R853H mutation showed a kinase activity identical to cells carrying wildtype  
91 *NDEL1-PDGFRB*. The phosphorylation level of PDGFR $\beta$  and one of its downstream  
92 targets, Erk, which is activated via the Ras-pathway<sup>12</sup>, was higher in Ba/F3-NDEL1-  
93 PDGFRB cells carrying the H657K or D850E mutations in comparison to wildtype or  
94 R853H-carrying fusion gene constructs (Fig.2B).

95 The *in vitro* responsiveness of Ba/F3-NDEL1-PDGFRB cells to different TKIs of type-I  
96 (dasatinib, midostaurin, pacritinib) and type-II (imatinib, nilotinib, sorafenib) was  
97 determined by MTT assays. Cells expressing wildtype *NDEL1-PDGFRB* were  
98 sensitive to all TKIs tested (Fig.2A). By contrast, proliferation of Ba/F3 cells carrying  
99 the D850E mutation in the *NDEL1-PDGFRB* gene could only be inhibited by the  
100 indicated type-I TKIs at sub-micromolar concentrations (Fig.2A). The observation of

101 TKI resistance apparently induced by the D850E mutation in the kinase domain of  
102 PDGFR $\beta$  was in contrast to the same amino acid exchange at the corresponding site  
103 in PDGFR $\alpha$  (D842E)<sup>13</sup>. This finding raised questions regarding important structural  
104 differences between the two highly homologous RTKs. While PDGFR $\beta$  displays an  
105 arginine in the +3 position to the mutation site (R853), PDGFR $\alpha$  has the much shorter  
106 and less basic histidine in the corresponding position (H845) (Fig.1H). It appeared  
107 conceivable therefore that interaction between the side chains of R853 and E946 in  
108 the mutant PDGFR $\beta$  TKD could stabilize the active conformation in the presence of  
109 H657K or D850E mutations, thus mediating resistance to type-II TKIs. To address  
110 this notion, the mutation R853H was introduced into *NDEL1-PDGFRB* constructs,  
111 thus mimicking the sequence of the A-loop in the PDGFR $\alpha$  TKD (Fig.1H). In line with  
112 the properties of the D842E mutation in the FIP1L1-PDGFR $\alpha$  fusion, this change  
113 restored the TKI type-II sensitivity of cells carrying one of the activating mutations,  
114 H657K or D850E, in *NDEL1-PDGFR $\beta$*  (Fig.2).

115 The position of the newly identified mutation D850E in PDGFR $\beta$  corresponds to well-  
116 known mutation sites within the activation loop of other members of the PDGFR-RTK  
117 family including c-KIT (D816)<sup>14</sup>, PDGFR $\alpha$  (D842)<sup>13, 15</sup>, and FLT3 (D835)<sup>5</sup> (Fig.1H).  
118 Mutations converting the aspartate residue at the indicated positions into a bulky  
119 hydrophobic residue were shown to mediate resistance to type-II TKIs<sup>5, 15, 16</sup>.  
120 Structural studies revealed that the interaction of the residues D816 in c-KIT and  
121 D835 in FLT3 with the residue at the +3 position (N819 in c-KIT and S838 in FLT3)  
122 may maintain the auto-inhibitory inactive conformation of the A-loop<sup>6</sup>. Notably,  
123 clinically relevant activating mutations D816V in c-KIT and D835V/Y in FLT3  
124 converting the aspartate into a residue with bulky hydrophobic or aromatic side chain  
125 would disrupt the hydrophilic interactions with the corresponding residue at +3

126 position. However, a conversion of aspartate to glutamate, representing an exchange  
127 between two hydrophilic and negatively charged amino acids at this position, has  
128 never been associated with resistance to type-II TKIs<sup>5, 13, 16</sup>. In marked contrast to the  
129 clinical and *in vitro* data presented, the identical mutation at the corresponding site in  
130 the tyrosine kinase domain of PDGFR $\alpha$  (D842E) in the fusion gene *FIP1L1-PDGFR* $\alpha$   
131 associated with chronic eosinophilic leukemia did not cause any significant increase  
132 in IC<sub>50</sub> values of the type-II TKIs imatinib, nilotinib, and sorafenib<sup>13</sup> (Fig.2A). Similarly,  
133 the same mutation at the corresponding site of FLT3 associated with acute myeloid  
134 leukemia, D835E, did not significantly increase the IC<sub>50</sub> to the type-II TKIs sunitinib  
135 and sorafenib<sup>5, 16</sup> but enhanced the kinase activity of FLT3, and mediated growth  
136 factor-independent proliferation of the murine hematopoietic cell line Ba/F3<sup>17</sup>.  
137 However, although these analogies are in line with the enhanced kinase activity of  
138 the D850E PDGFR $\beta$  mutant, they do not explain the observed resistance to type-II  
139 TKIs. In this regard, it is important to examine the protein model in the context of  
140 intramolecular interactions specific for PDGFR $\beta$  TKD. Protein modelling of the  
141 PDGFR $\beta$  TKD suggested that the residue in +3 position, R853, which differs from  
142 corresponding sites in all other RTKs of the PDGFR family, mediates a critical amino  
143 acid interaction stabilizing the A-loop in the active conformation, thereby preventing  
144 the interaction of type-II TKIs with their target sites in the kinase domain. This notion  
145 was confirmed by mutating R853 to histidine, the amino acid present at the  
146 corresponding site in PDGFR $\alpha$ , which decreased the kinase activity and restored  
147 sensitivity of NDEL1-PDGFR $\beta$  with D850E or H657K to type-II TKIs. The findings not  
148 only confirm the important role of R853 in establishing the resistant phenotype of the  
149 mutant *NDEL1-PDGFR $\beta$* , but also underline the potential of protein modelling for  
150 prediction of sensitivity and resistance to TKI treatment. The data presented provide

151 new insights into specific amino acid interactions in mutant RTKs which are of clinical  
152 relevance for improved selection of appropriate TKI treatment.

### 153 **Acknowledgement**

154 This work was supported by the Austrian Science Fund (FWF), SFB Grants F4705-  
155 B20 (T.L.), F4704-B20 (P.V.), and F4711-B20 (G. S.-F.).

### 156 **Conflict of Interest**

157 The authors declare no conflict of interests.

## 158 **References**

- 159 1. Valent P, Klion AD, Horny HP, Roufosse F, Gotlib J, Weller PF, *et al.* Contemporary consensus  
160 proposal on criteria and classification of eosinophilic disorders and related syndromes. *The*  
161 *Journal of allergy and clinical immunology* 2012 Sep; **130**(3): 607-612 e609.
- 162  
163 2. Arber DA, Orazi A, Hasserjian R, Thiele J, Borowitz MJ, Le Beau MM, *et al.* The 2016 revision  
164 to the World Health Organization classification of myeloid neoplasms and acute leukemia.  
165 *Blood* 2016 May 19; **127**(20): 2391-2405.
- 166  
167 3. Cheah CY, Burbury K, Apperley JF, Huguet F, Pitini V, Gardembas M, *et al.* Patients with  
168 myeloid malignancies bearing PDGFRB fusion genes achieve durable long-term remissions  
169 with imatinib. *Blood* 2014 Jun 5; **123**(23): 3574-3577.
- 170  
171 4. Garuti L, Roberti M, Bottegoni G. Non-ATP competitive protein kinase inhibitors. *Current*  
172 *medicinal chemistry* 2010; **17**(25): 2804-2821.
- 173  
174 5. Smith CC, Lin K, Stecula A, Sali A, Shah NP. FLT3 D835 mutations confer differential resistance  
175 to type II FLT3 inhibitors. *Leukemia* 2015 Jun 25.
- 176  
177 6. Mol CD, Dougan DR, Schneider TR, Skene RJ, Kraus ML, Scheibe DN, *et al.* Structural basis for  
178 the autoinhibition and STI-571 inhibition of c-Kit tyrosine kinase. *The Journal of biological*  
179 *chemistry* 2004 Jul 23; **279**(30): 31655-31663.
- 180  
181 7. McTigue M, Murray BW, Chen JH, Deng YL, Solowiej J, Kania RS. Molecular conformations,  
182 interactions, and properties associated with drug efficiency and clinical performance among  
183 VEGFR TK inhibitors. *Proceedings of the National Academy of Sciences of the United States of*  
184 *America* 2012 Nov 6; **109**(45): 18281-18289.
- 185  
186 8. Illig CR, Manthey CL, Wall MJ, Meegalla SK, Chen J, Wilson KJ, *et al.* Optimization of a potent  
187 class of arylamide colony-stimulating factor-1 receptor inhibitors leading to anti-  
188 inflammatory clinical candidate 4-cyano-N-[2-(1-cyclohexen-1-yl)-4-[1-  
189 [(dimethylamino)acetyl]-4-piperidinyl]phenyl]-1H-imidazole-2-carboxamide (JNJ-28312141).  
190 *Journal of medicinal chemistry* 2011 Nov 24; **54**(22): 7860-7883.
- 191  
192 9. Eling C, Erben P, Walz C, Frickenhaus M, Schemionek M, Stehling M, *et al.* Novel imatinib-  
193 sensitive PDGFRA-activating point mutations in hypereosinophilic syndrome induce growth  
194 factor independence and leukemia-like disease. *Blood* 2011 Mar 10; **117**(10): 2935-2943.
- 195  
196 10. Donald JE, Kulp DW, DeGrado WF. Salt bridges: geometrically specific, designable  
197 interactions. *Proteins* 2011 Mar; **79**(3): 898-915.
- 198  
199 11. Wachter K, Kowarz E, Marschalek R. Functional characterisation of different MLL fusion  
200 proteins by using inducible Sleeping Beauty vectors. *Cancer letters* 2014 Oct 1; **352**(2): 196-  
201 202.



- 202  
203 12. Demoulin JB, Essaghir A. PDGF receptor signaling networks in normal and cancer cells.  
204 *Cytokine & growth factor reviews* 2014 Jun; **25**(3): 273-283.
- 205  
206 13. von Bubnoff N, Gorantla SP, Engh RA, Oliveira TM, Thone S, Aberg E, *et al.* The low frequency  
207 of clinical resistance to PDGFR inhibitors in myeloid neoplasms with abnormalities of PDGFRA  
208 might be related to the limited repertoire of possible PDGFRA kinase domain mutations in  
209 vitro. *Oncogene* 2011 Feb 24; **30**(8): 933-943.
- 210  
211 14. Sotlar K, Fridrich C, Mall A, Jaussi R, Bultmann B, Valent P, *et al.* Detection of c-kit point  
212 mutation Asp-816 --> Val in microdissected pooled single mast cells and leukemic cells in a  
213 patient with systemic mastocytosis and concomitant chronic myelomonocytic leukemia.  
214 *Leukemia research* 2002 Nov; **26**(11): 979-984.
- 215  
216 15. Weisberg E, Wright RD, Jiang J, Ray A, Moreno D, Manley PW, *et al.* Effects of PKC412,  
217 nilotinib, and imatinib against GIST-associated PDGFRA mutants with differential imatinib  
218 sensitivity. *Gastroenterology* 2006 Dec; **131**(6): 1734-1742.
- 219  
220 16. von Bubnoff N, Engh RA, Aberg E, Sanger J, Peschel C, Duyster J. FMS-like tyrosine kinase 3-  
221 internal tandem duplication tyrosine kinase inhibitors display a nonoverlapping profile of  
222 resistance mutations in vitro. *Cancer research* 2009 Apr 1; **69**(7): 3032-3041.
- 223  
224 17. Clark JJ, Cools J, Curley DP, Yu JC, Lokker NA, Giese NA, *et al.* Variable sensitivity of FLT3  
225 activation loop mutations to the small molecule tyrosine kinase inhibitor MLN518. *Blood*  
226 2004 Nov 1; **104**(9): 2867-2872.
- 227  
228  
229

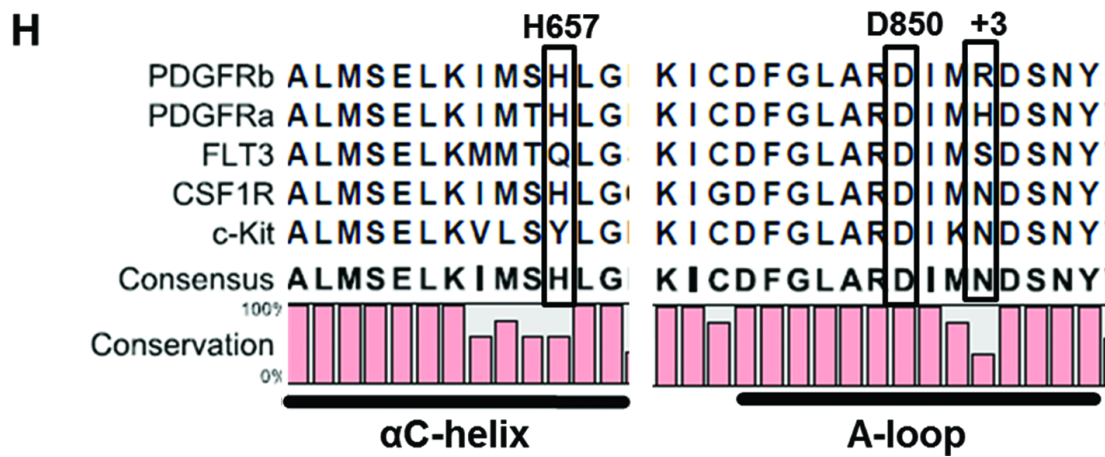
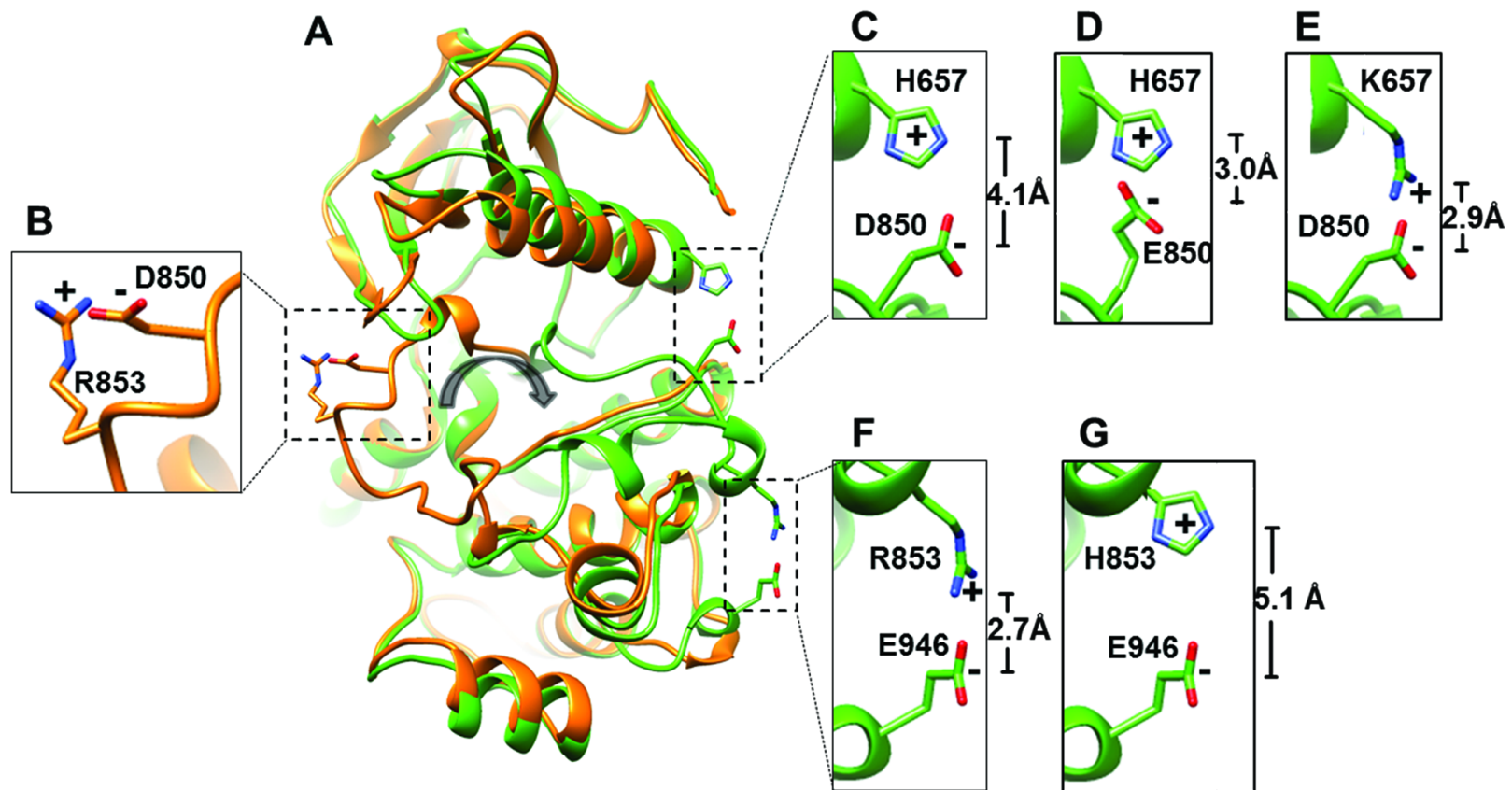
## 230 **Figure Legends**

### 231 **Figure 1. Protein models of the PDGFR $\beta$ TKD structure**

232 (A) The modelled DFG-*out* (orange) and DFG-*in* (green) conformations of PDGFR $\beta$  TKD are  
233 displayed. The zoom-in windows show the relevant stabilizing electrostatic interactions with the  
234 corresponding distances between charges: (B) D850-R853 in the DFG-*out* model; (C) H657-D850, (D)  
235 H657-E850, (E) K657-D850, (F) R853-E946, and (G) H853-E946 in the DFG-*in* model. Oxygen atoms  
236 carrying negative charge are marked in red, nitrogen atoms carrying positive charge in blue. The grey  
237 arrow in the center indicates rotation of the A-loop upon transition from inactive to active state. (H)  
238 Sequence alignment of RTKs from the PDGFR family depicting the region covering  $\alpha$ C-helices and A-  
239 loops of PDGFR $\alpha$ , PDGFR $\beta$ , FLT3, CSF-1R, and c-Kit.

### 240 **Figure 2. TKI-responsiveness of wildtype and mutant *NDEL1-PDGFRB* genes**

241 (A) Displayed are IC<sub>50</sub> values of different TKIs against Ba/F3 cells expressing wildtype (wt) or mutant  
242 NDEL1-PDGFR $\beta$  fusion proteins. The corresponding IC<sub>50</sub> values for Ba/F3 expressing FIP1L1-  
243 PDGFR $\alpha$  WT and D842E are given for comparison. (B) Western blot analysis of Ba/F3 cells  
244 transduced with wildtype or mutant (R = R853H, H = H657K, HR = H657K/R853H, D = D850E, and  
245 DR = D850E/R853H) *NDEL1-PDGFRB* genes. The phosphorylation levels of NDEL1-PDGFR $\beta$  at  
246 Y751 and Y857, and Erk are displayed. Shown are also the total expression levels of NDEL1-  
247 PDGFR $\beta$ , Erk, and the control gene Gapdh upon mock treatment for 4 h with DMSO (indicated by “-“)  
248 or with 100 nM nilotinib (indicated by “+”).



**A**

	TKI	NDEL1-PDGFR $\beta$					FIP1L1-PDGFR $\alpha$		
		WT	R853H	D850E	DR	H657K	HR	WT	D842E
Type II	IMA	80	50	>5000	15	>5000	15	2	4
	NIL	90	40	2200	12	2100	10	8	12
	SOR	40	30	2100	15	1900	10	1	2
Type I	DAS	20	10	25	12	25	10	7	N/A
	MID	25	20	15	15	10	12	30	N/A
	PAC	30	25	10	12	15	13	N/A	N/A

**B**